Measurement of Fast Transients in Nb_3Sn Magnets by Using a Static Harmonic-Coil

Piotr Rogacki, Lucio Fiscarelli, Arnaud Devred, *Senior Member, IEEE*, and Stephan Russenschuck

***Abstract*—An induction-coil magnetometer has been produced at CERN to determine the location of an incipient quench in the HL-LHC Nb_3Sn inner-triplet quadrupoles. The instrument, known as a quench-antenna, allows the measurement of the position and propagation of quenches with a reduced number of acquisition channels. This is possible because four layers of nested coils are designed to be sensitive only to the normal and skew sextupole and octupole components. Moreover, the magnetometer allows the study of fast magnetic transients due to flux jumps observed during the ramping of Nb_3Sn superconducting accelerator magnets. This paper presents the observation and characterization of flux jumps during powering ramps similar to machine operations. Spatial and temporal distributions of flux jumps are derived from the induced voltages in the quench-antenna as a function of the transport current. Modeling flux jumps as traveling magnetic moments allows the reconstruction of the effect in terms of position and magnitude and, thus, an estimation of the impact on the magnetic field quality.**

***Index Terms*—Accelerators, flux jumps, induction coils, magnets, Nb_3Sn.**

I. Introduction

FUTURE accelerators require magnetic field strengths not achievable with the widely-used superconductors based on Nb-Ti [1]. Nb_3Sn technology is one of the most promising approaches for achieving magnetic fields that exceed 10 T [2]. Its first use in an accelerator is in the scope of the High-Luminosity Large Hadron Collider project (HL-LHC), and in particular in its inner-triplet quadrupoles (MQXF) [3]. Besides challenges related to the mechanical properties of the reacted material, cables based on this superconductor exhibit more thermo-magnetic instabilities (flux jumps) compared with Nb-Ti ones [4]. Understanding the behavior of these instabilities and their effect on the magnetic field quality is essential for operating the magnets in the accelerators [5].

A measurement instrument based on nested harmonic coils, similar to the one described in [6], was recently developed at CERN for quench-start localization in the transverse plane. Moreover, the instrument allows the investigation of other fast transients, such as flux jumps and conductor vibrations. Fig. 1 shows the typical signatures of the three types of transients, as measured with the harmonic coils.

Received 25 September 2024; revised 24 January 2025; accepted 27 February 2025. Date of publication 11 March 2025; date of current version 20 March 2025. *(Corresponding author: Piotr Rogacki.)*

The authors are with CERN, CH-1211 Geneva, Switzerland (e-mail: p.rogacki@cern.ch).

Color versions of one or more figures in this article are available at https://doi.org/10.1109/TASC.2025.3550313.

Digital Object Identifier 10.1109/TASC.2025.3550313

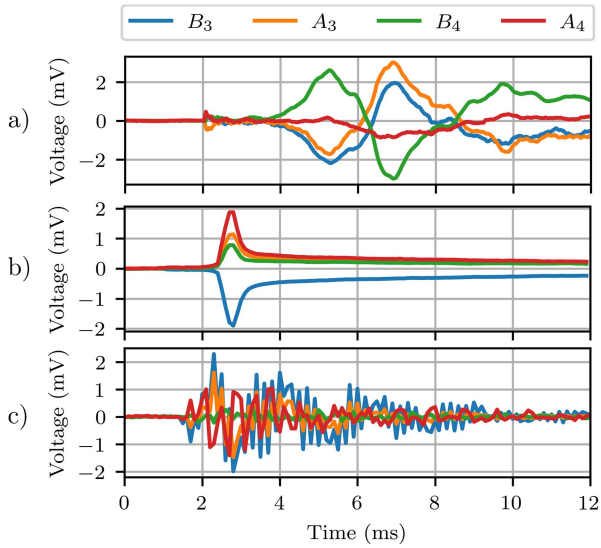

Fig. 1. Examples of different types of transient observed by the quench antenna during an excitation ramp in the MQXFB03 quadrupole: (a) Quench onset and propagation, (b) flux jump, and (c) mechanical vibrations. B_3 and A_3, and B_4 and A_4 correspond to coils sensitive to normal and skew sextupole, and normal and skew quadrupole, respectively.

II. Complex Formulation

The localization of the source of a magnetic-field transient is based on the assumption that it can be modeled as a magnetic moment [7]. When the flux is measured with pickup coils that are significantly longer than the source of the magnetic moment, a two-dimensional field reconstruction is sufficient. In its simplest variant, a magnetic dipole moment creates a field pattern that can be well expressed as a set of complex field harmonics [8]:

$$C_n = B_n + \mathrm{i}A_n = m\frac{\mathrm{i}\mu_0 n}{2\pi}\frac{e^{\mathrm{i}\alpha}}{z_c^2}\left(\frac{r_0}{z_c}\right)^{n-1} \tag{1}$$

where $n = 1, 2, 3, \ldots$ is the multipole order, m is the transverse magnetic moment ($[m] = \mathrm{Am}$), α is the orientation of the moment, z_c is the location of the moment center in the complex plane, and r_0 is the reference radius for expressing the field multipoles.

By using four sets of coils, each exclusively sensitive to a single multipole, we can analytically solve the inverse problem and retrieve the four parameters of the magnetic moment. A convenient choice are the two next higher-order complex multipoles with respect to the main quadrupole component. Here, $C_3 = B_3 + \mathrm{i}A_3$ and $C_4 = B_4 + \mathrm{i}A_4$ yield the location of the

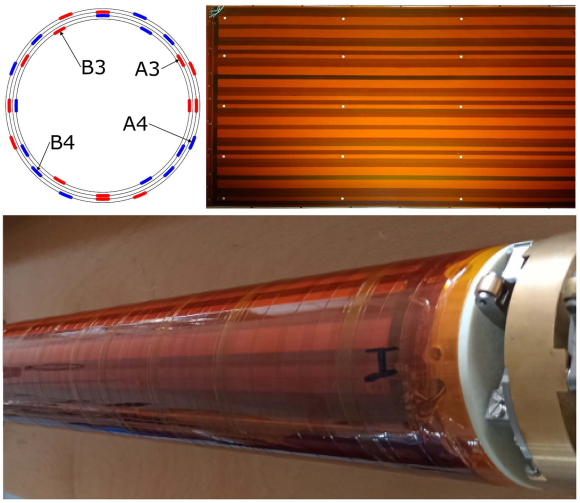

Fig. 2. Quench antenna during assembly; Two PCBs on each mandrel. The top-left corner shows the winding cross-section, and the top-right shows the PCB before wrapping.

source in the complex plane by:

$$z = x + iy = \frac{4}{3}\frac{C_3}{C_4} r_0 \ . \tag{2}$$

The advantage of using the complex formulation with analytic solution compared to a numerical one is obvious when, instead of relatively short time spans for quench localization, there is a much longer acquisition time comprising an entire ramp-up to the magnet's nominal current. In the case of the HL-LHC inner triplets, this implies approximately 15 minutes of acquisition at a 10 kHz sampling rate, resulting in a large data set containing a significant number of events.

III. Transducer Design

A possible way to create a set of coils with enough freedom for the winding arrangement and alignment on a cylindrical mandrel, is by using flexible PCB technology [9]. Theoretically, a continuous cosine-theta-like distribution of windings would provide sensitivity to one multipole only. However, due to manufacturing constraints, this is not completely achievable.

Since the presented transducer has to cover the entire 8-meter length of the MQXF magnets, it consists of a chain of 12 flexible PCBs with 4 nested coils, 600 mm each. Multiple segments also allow us to estimate the longitudinal location of the transient with a limited resolution. To minimize the gaps between them and provide space for connections and alignment pins, we chose a rectangular winding shape; see Fig. 2, top-left corner. Nevertheless, with such an arrangement, the sensitivities to unwanted higher-order field harmonics can be kept below 3% , considering that the magnetic moment is located at least 3/2 of the quench antenna's coil radius away from the transducer axis. This is always true in MQXF magnets with an aperture radius of 75 mm for the 50 mm coil radius of the quench antenna. This translates to a ±5 mm transversal error in the worst-case scenario, which is an acceptable uncertainty for the quench localization in the magnet cross-section. The uncertainty has been verified experimentally by using a precisely positioned

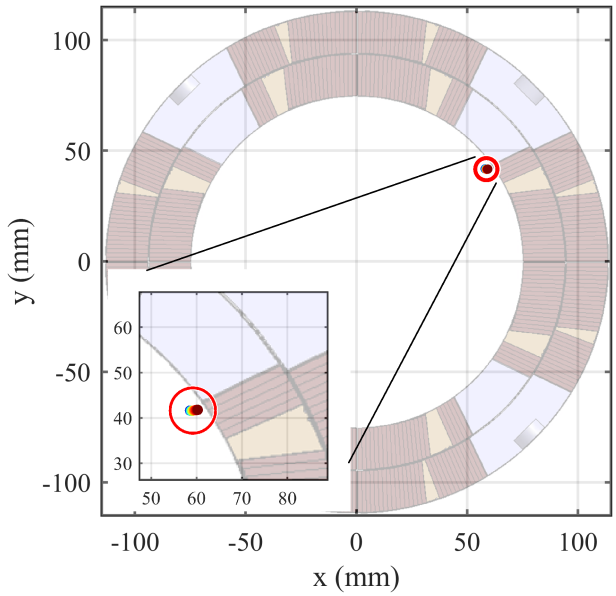

Fig. 3. Quench localization in the transversal cross-section of an MQXF magnet. The brown rectangles represent the superconducting cable, and the silver and beige sectors represent poles and coil wedges, respectively. The red circle indicates the expected uncertainty.

synthetic moment made of a small solenoid. Fig. 2 shows the final system assembly.

A localization example of a single event, the same quench as in Fig. 1(a), is shown in Fig. 3. As the induction coils are sensitive to the change of flux linkage, the acquired voltages are integrated and multiplied by coil sensitivities to obtain the field multipoles (C_3 and C_4) generated by the magnetic moment, in Tesla. Feeding the integrated values into (2) yields the location of the moment directly. Several samples around the first peak of the signal (approx. 4.5 ms to 5.5 ms in Fig. 1(a)) are used to provide an estimation of the localization stability, which equals 2 mm in the presented case.

IV. Flux Jump Propagation

The instrument also allows the analysis of the flux jumps in terms of localization and propagation velocity. The first observation, confirming and extending previous findings [10], is that the flux jumps propagate along the conductors of the magnet coils. Fig. 4 shows an example of a flux jump propagation as seen by the harmonic coils sensitive to the normal sextupole component. The plot refers to a current ramp at 4.5 K operation temperature at which the effect is more pronounced than at 1.9 K. From these measurements, we can retrieve propagation velocities in the range of 350–700 m/s at 1.9 K, and slightly higher 500–900 m/s at 4.5 K. The transversal localization further supports the assumption that the flux jump follows the conductor on multiple full turns through the coil-heads [10].

A similar procedure as for the quench localization is followed to locate a single flux jump. The integration of the voltage signal is started at the beginning of the signal rise and stopped at the first maximum, when the propagating front has left the induction-coil segment.

After leaving the induction-coil segment, the propagating front is immediately visible in the next one. The transversal

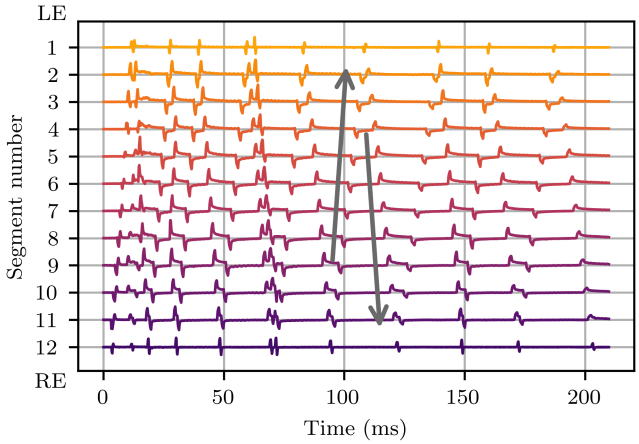

Fig. 4. Plot showing the outputs from all the quench antenna segments in a ramp to the nominal at 4.5 K. Each line is a signal from one of the 12 normal sextupole coils. The left scale shows the PCB number along the magnet, LE and RE stand for lead-end and return-end of the magnet, respectively. The gray arrows highlight the same flux jump propagating along the magnet. The magnet current is approximately 3 kA.

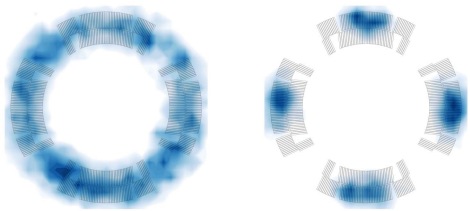

Fig. 5. Spatial distribution of flux jumps in the MQXF magnet cross-section for high (b) and low (a) magnetic flux density ranges (peak field provided at the inner coil radius of 75 mm). (a) 1.9 K, 1.3–4 T. (b) 1.9 K, 4–5.3 T.

location remains approximately the same. After traversing the magnet head, the front continues in the other longitudinal direction, and its transversal location moves to the other side of the coil turn (or pole). Initially, several flux jumps are present at the same time in different locations. However, after approximately 75 ms only one flux jump remains and continues to propagate multiple times through the magnet.

V. Flux Jump Distribution

The harmonic quench antenna can also be used to observe the development of the spatial distribution of the flux jumps in the magnet cross-section as a function of the magnet current or field. Fig. 5 shows how the distribution changes for different current ranges. The distributions exhibit a shift towards the inside of the aperture. This could indicate that flux jumps must be modeled with a more complex current re-distribution than a magnetic dipole. All the results below have been corrected by an experimentally determined factor of 1.25, which brings the distributions well within the conductor domain, where it is expected.

The first visible characteristic is that the flux jumps are distributed more evenly for low current levels and tend to concentrate at the mid-planes with increasing current. This is expected since flux jumps are more likely to happen at lower fields and less at high field levels [11], [12]. For MQXF magnets,

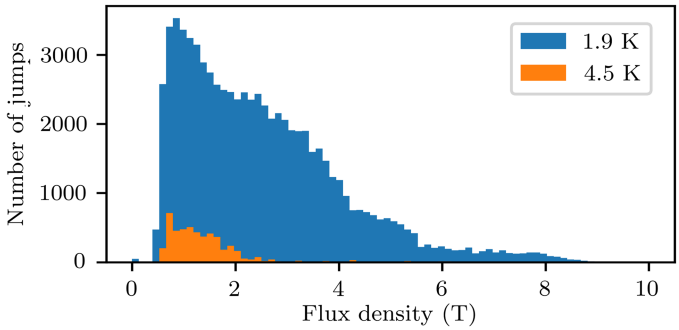

Fig. 6. Histogram showing the number of the flux jumps as a function of magnetic flux density (peak field at the inner coil radius of 75 mm). The events have been filtered to include only the ones in the radial domain of 65 to 125 mm. The histogram bin size is 0.13 T.

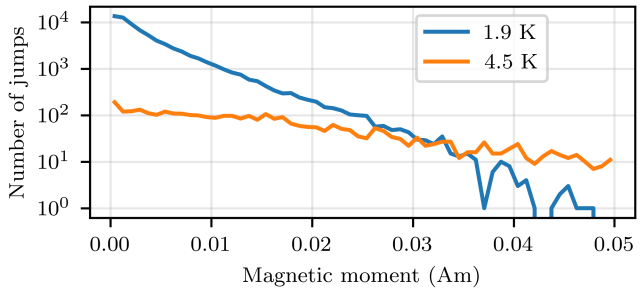

Fig. 7. Distribution of flux jumps as a function of measured magnetic dipole moment strength for 1.9 K and 4.5 K. The events have been filtered to include only the ones in the radial domain of 65 to 125 mm. Each point corresponds to a bin size of 8×10^{-4} Am.

at 1.9 K, flux jumps persist until 8 kA and only after 6 kA their transition to the mid-planes becomes apparent. At 4.5 K, this happens already around 2–3kA, and the flux jump frequency is significantly reduced before 6 kA.

This temperature dependence is visible in Fig. 6, which also shows that there are notably fewer flux jumps at 4.5 K. They are, however, larger in magnitude; see Fig. 7 for a qualitative comparison showing the flatter distribution for the higher temperature. While not shown in the plot, the longitudinal distribution of the flux jumps is approximately uniform, with no quench antenna segments recording significantly different signals.

VI. Effects on the Field Quality

We can now estimate the effect of the flux jumps on the magnetic field quality during the current ramp. Since the measurements indicate that the longitudinal distribution of flux jumps is nearly uniform, we can focus on the central field without loss of generality and assume that the local 2D effects represent the average behavior over the entire magnet length.

Due to their large numbers, there is a significant probability of multiple flux jumps intercepted by the same quench antenna segment at different transversal locations. In such cases, the single magnetic moment model used to localize and characterize the phenomenon no longer applies. Therefore, to better characterize the effect on the magnetic field, we chose a subset of flux jumps that are well separated from others and can provide more robust data for the distribution. The flux jump was included in the subset if the signals decayed to less than 0.1 mV before the jump onset,

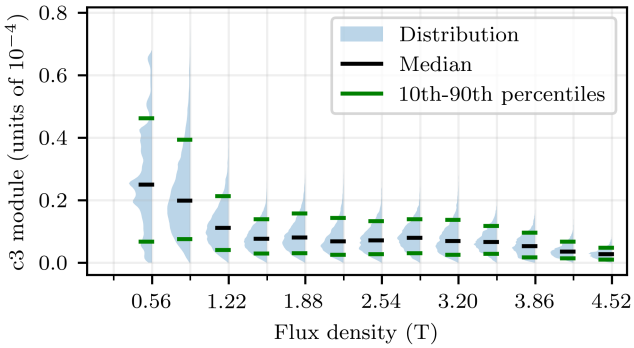

Fig. 8. Distributions of the module of the flux-jump-generated sextupole, normalized to the main quadrupole field, provided at the reference radius of 50 mm. Each distribution encompasses a field range of approximately 0.33 T (peak field at the inner coil radius of 75 mm).

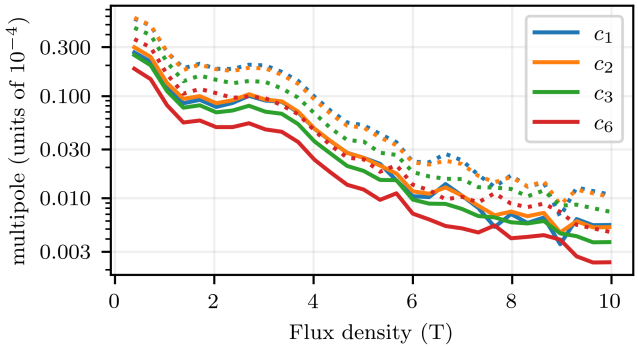

Fig. 9. Median (solid) and 90th percentile (dotted) values for field multipoles generated by the flux jumps.

and the tail had at least 2 ms of monotonic decay. The resulting subset contains approximately 8000 jumps, which corresponds to 3% of the full subset used for the qualitative study. Assuming these distributions apply to all the events, we can calculate the global effects on all field harmonics. Henceforth, we will rely on the quench antenna to provide two complex field multipoles directly.

First, let us consider the relation of the multipole fields excited by a magnetic dipole moment. Starting from (1), we select C_3 as the reference multipole to which we normalize all others,

$$\frac{C_n}{C_3} = \frac{n}{3}\left(\frac{r_0}{z_c}\right)^{n-3}. \tag{3}$$

Considering that flux jumps can appear only inside the coils, we can establish bounds on the variation of these normalized multipoles. For the sources located within the radial domain of interest (75–115 mm), the higher-order multipoles are never exceeding the C_3 component, and the lower-order ones are no more than 1.75 times larger. The latter is the case for the events located in the outermost region of the coils.

The first step is to investigate the third and fourth-order multipoles. To account for overlapping events, we integrate the acquired voltages over longer time spans of several seconds, instead of just a few milliseconds used for characterizing a single flux jump. Longer integration times are to be avoided due to the varying acquisition offsets and the resulting drift. Due to the nearly uniform distribution of the moments, the multipoles never diverge in the longer term. The largest sources of any instantaneous disturbance are the *cascade* events, where many flux jumps happen in quick succession. Moreover, the effect of several such events on a given harmonic content can be compounded before the recovery, which usually takes a few seconds.

We cannot directly model such a scenario as a magnetic moment, as not all the jumps occur in the same transversal location, and their signals effectively obscure each other. However, we can estimate the distribution of the field harmonics produced by flux jumps using the relation between the multipoles in (3), the spatial distributions of the moments (Fig. 5), and the distributions of C_3 integrated over periods of 25 s. There is no significant difference between 5 s to 50 s, but beyond that the drift becomes non-negligible. Fig. 8 shows the evolution of the c_3 multipole (normalized to the main quadrupole field: $c_3 = \frac{C3}{|C2|}$).

By combining these distributions with the respective ones for the radius, we can obtain similar distributions for each field multipole. The medians and the 90th percentiles of these distributions are shown in Fig. 9. This is the worst-case scenario, which assumes a magnetic dipole moment. Calculations indicate that the more complex current re-distributions always result in a reduction of the normalized dipole and quadrupole components at the cost of a slight increase of high-order multipoles. The normalized field multipoles generated by the flux jumps can reach 0.7 units at low field levels. However, they decrease below 0.1 unit at approximately 4 kA. In general, the generated multipole strength decreases with its order. The C_1 is particularly interesting as it relates to the displacement of the magnetic axis. Even in the worst-case scenario at low currents, the axis error is lower than 3 µm in the studied magnet.

VII. Conclusion

In this paper, we have shown that the multipole-sensitive coil array, based on 4 layers of harmonic coils, allows us to observe and characterize dynamic effects due to flux jump instabilities and estimate their impact on the field quality in Nb_3Sn magnets. While for the HL-LHC inner-triplet magnets the effects can be considered negligible [5], these instabilities could noticeably affect the performance of accelerators based fully on Nb_3Sn superconductors. Furthermore, these results confirm the need for more sophisticated quench detection mechanisms - in the low-current regime the signals generated by flux jumps are larger than the safe quench detection limits for high currents. Using several successive, current dependent thresholds is necessary to avoid premature quench protection firing [13]. Since the flux jumps decrease in number and amplitude at higher fields, this approach should also be sufficient.

Moreover, assuming that flux jumps create a magnetic dipole moment due to the local redistribution of currents in the Rutherford-type cable does not model the phenomena fully, resulting in a shift of the momenta toward the inner coil radius. Further analysis of the measured data could yield more insight into the phenomenology or the confirmation of more sophisticated models of flux jump instabilities, which would lead to a further refined estimation of the effects on the field. Furthermore, adding more multipole-sensitive coils to the set could provide additional information for discerning the model order of the underlying phenomenon.

REFERENCES

[1] A. Abada, M. Abbrescia, and S. S. AbdusSalam, "FCC-hh: The hadron collider," *Eur. Phys. J. Special Topics*, vol. 228, no. 4, pp. 755–1107, Jul. 2019, doi: 10.1140/epjst/e2019-900087-0.

[2] A. Ballarino and L. Bottura, "Targets for R&D on Nb_3Sn conductor for high energy physics," *IEEE Trans. Appl. Supercond.*, vol. 25, no. 3, Jun. 2015, Art. no. 6000906. [Online]. Available: https://ieeexplore.ieee.org/abstract/document/7017491

[3] P. Ferracin et al., "Development of MQXF: The Nb_3Sn low-β quadrupole for the HiLumi LHC," *IEEE Trans. Appl. Supercond.*, vol. 26, no. 4, Jun. 2016, Art. no. 4000207.

[4] B. Bordini et al., "Voltage spikes in Nb_3Sn and NbTi strands," *IEEE Trans. Appl. Supercond.*, vol. 16, no. 2, pp. 366–369, Jun. 2006. [Online]. Available: https://ieeexplore.ieee.org/document/1642864

[5] J. C. d. Portugal, R. Tomas, L. Fiscarelli, D. Gamba, and M. Martino, "Impact of flux jumps in future colliders," *Phys. Rev. Accelerators Beams*, vol. 23, no. 1, Jan. 2020, Art. no. 011001, doi: 10.1103/PhysRevAccelBeams.23.011001.

[6] T. Ogitsu et al., "Quench antenna for superconducting particle accelerator magnets," *IEEE Trans. Magn.*, vol. 30, no. 4, pp. 2273–2276, Jul. 1994.

[7] K. Sasaki, T. Ogitsu, N. Ohuchi, and K. Tsuchiya, "Study of quench propagation with quench antennas," *Nucl. Instrum. Methods Phys. Res. Sect. A: Accelerators, Spectrometers, Detectors Assoc. Equip.*, vol. 416, no. 1, pp. 9–17, Oct. 1998. [Online]. Available: https://linkinghub.elsevier.com/retrieve/pii/S0168900298006172

[8] S. Russenschuck, *Field Computation for Accelerator Magnets: Analytical and Numerical Methods for Electromagnetic Design and Optimization*. Weinheim, Chichester: Wiley-VCH, 2010.

[9] J. DiMarco et al., "A full-length quench antenna array for MQXFA production series quadrupole magnet testing," *IEEE Trans. Appl. Supercond.*, vol. 31, no. 5, Aug. 2021, Art. no. 9500705. [Online]. Available: https://ieeexplore.ieee.org/document/9390328

[10] M. Marchevsky et al., "Axial-field magnetic quench antenna for the superconducting accelerator magnets," *IEEE Trans. Appl. Supercond.*, vol. 25, no. 3, Jun. 2015, Art. no. 9500605. [Online]. Available: https://ieeexplore.ieee.org/document/7029677/authors#authors

[11] S. Feher et al., "Sudden flux change studies in high field superconducting accelerator magnets," *IEEE Trans. Appl. Supercond.*, vol. 15, no. 2, pp. 1591–1594, Jun. 2005. [Online]. Available: https://ieeexplore.ieee.org/document/1439951/?arnumber=1439951

[12] S. Rahimzadeh-Kalaleh, G. Ambrosio, G. Chlachidze, C. Donnelly, and M. Tartaglia, "Analysis of voltage spikes in superconducting Nb_3Sn magnets," *IEEE Trans. Appl. Supercond.*, vol. 19, no. 3, pp. 2442–2445, Jun. 2009. [Online]. Available: https://ieeexplore.ieee.org/document/4914762

[13] J. Steckert, R. Denz, S. Mundra, T. Podzorny, J. Spasic, and D.-G. Vancea, "Application of the universal quench detection system to the protection of the high-luminosity LHC magnets at CERN," *IEEE Trans. Appl. Supercond.*, vol. 32, no. 6, Sep. 2022, Art. no. 4006305. [Online]. Available: https://ieeexplore.ieee.org/document/9714788